2012

Development of Thermoplastic Syntactic Foams For Energy Absorbing Applications

Aaron Siegel
University of Alabama at Birmingham

DEVELOPMENT OF THERMOPLASTIC SYNTACTIC FOAMS FOR ENERGY ABSORBING APPLICATIONS

by

AARON SIEGEL

DR. UDAY VAIDYA, CHAIR
DR. SELVUM PILLAY
DR. DERRICK DEAN

A THESIS

Submitted to the graduate faculty of The University of Alabama at Birmingham,
in partial fulfillment of the requirements for the degree of
Master of Science

BIRMINGHAM, ALABAMA

2012

DEVELOPMENT OF THERMOPLASTIC SYNTACTIC FOAMS FOR ENERGY ABSSORBING APPLICATIONS

AARON SIEGEL

MATERIALS SCIENCE AND ENGINEERING

ABSTRACT

Foams are often used for energy absorbing applications. Increasing a materials ability to absorb energy without increasing its weight is a difficult task. Foams have a low specific weight and high energy absorbing capabilities. Syntactic foams are unique in that their voids are created by the dispersion of hollow glass microspheres (HGMS) randomly distributed throughout a matrix. This allows the density, distribution of porosity, and consequently the weight of the material to be controlled. Thermoplastic syntactic polymer foam samples have been prepared at the Manufacturing, Processing, and Applications Development (MPAD) facility at the University of Alabama at Birmingham (UAB). Different thermoplastic polymers have been compounded with varying amounts of microspheres to create a new type of syntactic foam. Tests were conducted using various techniques including Non-Destructive Testing (NDT), quasi-static compression, low velocity impact (LVI), and dynamic compression tests with a Split Hopkinson Pressure Bar (SHPB). Scanning Electron Microscopy (SEM) was used to analyze fracture surfaces of compressed samples. Through the use of vibration analysis, the frequency response of foam beams to continuous excitation under free-free boundary conditions showed thermoplastic syntactic foams better energy absorbing capabilities than other materials.

Keywords: Syntactic foam, Microspheres, Compression, Thermoplastics, Energy Absorption.

DEDICATION

To my loving fiancé, parents, sisters, grandparents, family and friends for their support throughout my life and education. Thank you for always standing beside me.

ACKNOWLEDGMENTS

First the author would like to thank the Army Research Lab (ARL) for providing the funding for this project.The author would like to also acknowledge the time and effort spent on this project by others both students and professors. Firstly, I would like to thank my graduate committee Dr.Uday Vaidya, Dr.Selvum Pillay, and Dr.Derrick Dean. In addition, thank you to Dr.Balaji Thattaiparthasarathy for his efforts in the processing and production of the material for this research. Finally thank you to all other faculty and fellow graduate students for lending help when needed.

TABLE OF CONTENTS

page

LIST OF TABLES

Table *Page*

LIST OF FIGURES

Figure *Page*

1. INTRODUCTION

1.1. Background

Foams are a type of porous material that contains well distributed voids throughout. These voids are often referred to as cells and vary in shape and size. Typical foams can be closed (beaded polystyrene foam) or open cell (polyurethane foam), meaning cell walls are independent from one cell to the next or that cell walls are interconnected. Composite material containing spherical dispersoids as opposed to other conventional foams are called syntactic foams[1]. Syntactic foams are a special kind of particulate composite made with a binder and hollow filler. Syntactic or "syntaktikos" in Greek means an orderly dispersed system[2]. Syntactic foams are interesting materials because of their flexibility in manufacturing. Mechanical properties of a structure can be tailored to suit the intended application by varying the type of matrix or the type of hollow sphere. In this work thermoplastic polymer matrices are used with the same type of hollow glass microsphere (HGMS).

Applications of syntactic foams go back as early as the 1950's where they were used primarily in ship hulls, submarines, and buoys [2]. In the 1960's syntactic foams were used in deep water applications acting as pipe insulators [1]. These early syntactic foams consisted of epoxy binders and HGMS fillers.

With efforts focused on light weighting of structures for transportation and related industry, many are investigating the introduction of porosity into a material without sacrificing mechanical properties [3]. Just over the past three decades research on these mate-

rials has created a unique class of foams that use hollow spheres of many different types to create porosity. Hollow spheres are now made of glass, ceramic, and metals with applications ranging from aerospace, automotive, communications, biomedical, electronics, sporting, and other transportation industries[2-6].

1.2. Literature Review

This study is concerned with assessing thermoplastic polymer syntactic foam (TPSF) in areas of processing and mechanical properties for use as an energy absorbing material. Several areas of mechanical testing and material characterization were considered in the development of TPSF's.

1.2.1. Non-Destructive Evaluation

Non-Destructive Evaluation (NDE) is an important resource for characterizing composite materials. NDE is commonly used for detecting damage and defects in a structure and can also be used to detect porosity, matrix crazing or cracking, and delaminations [7].This method in conjunction with impact testing provides full understanding of the damage [8]. Ultrasonic C-Scan in through transmission mode was used to characterize specimens comprising syntactic foam of epoxy resin, glass fibers, and glass microspheres [7]. Ultrasonic NDE is also useful to characterize volume fraction of microspheres which is one of the determining factors of the foam's mechanical properties. Ultrasonics can help clarify if the processing method is adequate, i.e. evaluating the uniform dispersion of the microspheres in the matrix.

Another method of NDE includes the frequency response of the material to random noise produced by varying frequencies of vibration. Free vibration response is often

used to characterize the damping of a composite system [9]. Due to the viscoelastic nature of polymers they provide excellent damping and have been used extensively in composite materials. Some have used this method to successfully characterize materials from sandwich composites to glass-fiber reinforced composites [5, 10, 11]. This method is helpful in evaluating damping characteristics of different materials, the influence of matrix and filler properties, and damage assessments.

1.2.2. Dynamic Compression, Quasi-Static Compression, Low Velocity Impact

There have been few comprehensive studies of syntactic foams and their impact response. Most studies are concerned with mechanical properties at quasi-static conditions[12]. Syntactic foams have often been used in high strain rate applications and therefore require high strain rate testing by Split Hopkinson Pressure Bar (SHPB) or related apparatus. Recently there have been more studies that investigate the strain rate effects on epoxy based syntactic foams [3]. There is a large amount of literature available for these types of foams presented by Gupta and Woldesenbet [3, 6, 13-22].

Foams in general are unique in that there structure allows a large amount of energy to be absorbed due to something called a stress plateau [20]. There are three regions of a stress-strain curve for foam as shown in Figure 1. Region I is associated with the elastic response of the foam from cell bending. Region II, the plateau, is the zone where cells begin to bend and collapse and moves into region III where cell walls begin to touch and compact indicated by an increase in stress.

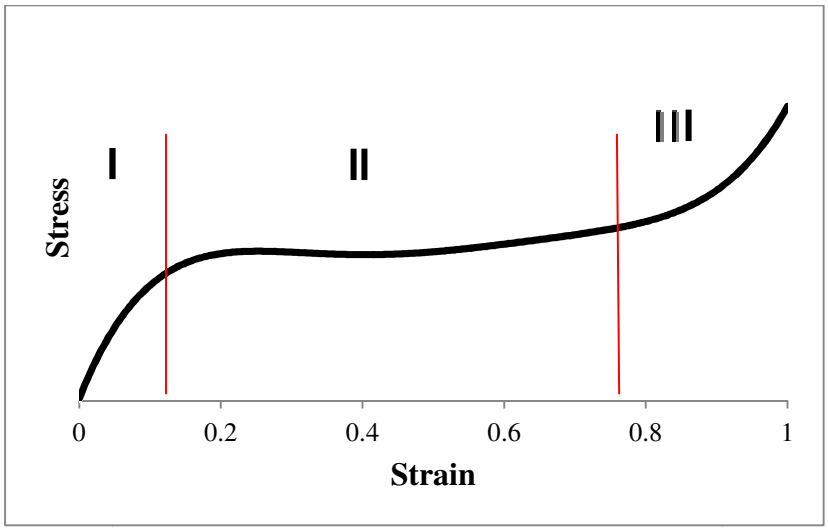

Figure 1 Typical stress-strain curve corresponding to the three regions of compression of foam

Quasi-static compression tests have been conducted with numerous results available. Typically an approximate crosshead speed of 1mm/min was used as well as the ASTM D-695-94 standardized test for compression of rigid plastics. It was shown that even under quasi-static conditions epoxy syntactic foams showed strain rate sensitivity[12]. Others investigated the effect of aspect ratio of samples for compression [12, 20]. To the best of the authors knowledge there is at least one work that has included a study on TPSF [23]. Polypropylene syntactic foam is tested under a confined compression conditions simulating a deep water environment [23]. This study includes acoustic emission and stress-strain data of a few different foams including polypropylene, polyurethane, and epoxy, however, for energy absorbing applications further investigations are required.

Comprehensive studies by Gupta and Woldesenbet [12, 16-21] investigate other factors influencing the mechanical properties of syntactic foam and coupled with high strain rate testing. Volume fraction of microspheres changes the density of syntactic foam

by increasing or decreasing the void content. Gupta and Woldesenbet introduced the concept of the radius ratio effect [6]. Equation 1 represents η, the radius ratio as a ratio of, r_1 the internal radius and r_o the external radius of the microsphere.

1

$$\eta = \frac{r_1}{r_o}$$

The effect of the radius ratio and volume fraction on mechanical properties was studied. As microsphere content increased compression strength and modulus decreased [20]. Volume fractions were said to have a dramatic effect on high strain rate properties of epoxy syntactic foams [20]. The high strain rate effects have been investigated now in a few papers [3, 12, 13, 17, 19, 20, 24]. In most cases peak stress increased as a function of increasing strain rate along with the modulus [3, 12, 20, 22]. The same was seen in polymeric structural foams [25]. From the literature cited in the above three statements it was gathered that strain rate effects are important in assessing the mechanical properties of any polymeric foam as polymers are rate sensitive. Low velocity impact (LVI) testing is a common method for testing sandwich composites, cores, and facesheets. Energy absorption is the main role for syntactic foam when used in a sandwich composite configuration. LVI has been conducted on epoxy vinyl ester resin syntactic foam showing stress and load endured by several specimens. It was found that the inclusion of glass microspheres in the material reduced both impact force and stress [26]. Metal foam core has also been studied with LVI drop weight tests providing the effectiveness of different face sheets. It was clearly seen in the force-time curves that the foam core has a significant effect on the energy absorption of the sandwich composite [5].

1.2.3. Microscopy

Scanning Electron Microscopy (SEM) complements quasi-static and high strain rate studies. SEM is useful for inspecting fracture surfaces before and after testing. A study by Gupta specifically examines the microscopy of syntactic foams and their fracture features[19]. Failure modes of syntactic foams changed with different specimen aspect ratios. Failure mode, either compression or shear, was decided based upon the number of microspheres fractured or intact on the fracture surface. If they were fractured there was failure under compression, otherwise it was failure due to shear.

1.2.4. Static and Dynamic Modeling

There have been a few attempts for modeling and simulation of syntactic foams. Static and dynamic simulations have been conducted by Gupta [15], Hobbs [27], Jhaver [28], Croop [29], and Abera [30]. Although they have modeled different types of syntactic foams, the most common mode of deformation for foams is under compression. As mentioned earlier, foam models show the three yield zones, an initial high stiffness zone, plateau zone, and compaction zone respectively. A study by Croop investigates the strain rate dependence of polyurethane foam using LS-DYNA to simulate the different strain rates [29]. From the Croop study, MAT_FU_CHANG (MAT83) in LS-DYNA was found to be the most appropriate material model for modeling the rate sensitivity of rate dependent polyurethane foam.

2. RESEARCH OBJECTIVES

The objectives of this research are to characterize thermoplastic polymer syntactic foams and their ability to absorb energy using a number of nondestructive, microscopy and characterization techniques. These include:

- Ultrasonic NDE for processing verification
- Vibration analysis to characterize blast/shockwave response
- Quasi-static and dynamic compression to capture rate sensitivity
- SEM analysis for investigation of failure modes and features
- Low velocity impact for blunt impact simulation
- Static/Dynamic modeling

Foams have many different applications and can be found in number of applications including automotive, transit, building infrastructure, military vehicles to name a few. For foams intended for use in energy absorbing applications the cells in the foam offer an extended region for stress dissipation. As stress increases cells collapse and allow the foam to absorb energy through plastic deformation of the cell. This region on a stress strain curve is known as the stress plateau. The larger the plateau is, the more energy that can be dissipated by the foam. For applications that require rigid and resilient foam, thermoplastic foams are a viable option. They provide flexibility in processing, manufacturing, and are light-weight durable materials. Many studies [3, 6, 13-15, 17, 19-

22, 30] have been performed using thermoset polymer such as epoxy vinyl ester and glass microspheres but there are few comprehensive studies of thermoplastic syntactic foams.

Although there is a variety of literature available covering the thermoset syntactic foams [3, 6, 13-15, 17, 19-22, 30], there has not been near as many studies done for TPSF's. Thermoplastic syntactic foams could be used for military, structural, or transportation applications acting as energy absorbing devices, light weighting, and other applications. Various non-destructive testing (NDT), impact scenarios, and compression tests have been aimed specifically at characterizing TPSF's for military applications. This study investigates the syntactic foam thermoplastic materials for their ability to reduce shock wave, blunt impact, high strain rate impact, compression, and the processing and production methods.

3. METHODS

3.1. Materials and Processing

TPSF's were produced at the University of Alabama at Birmingham's (UAB) Manufacturing, Processing and Development (MPAD) center (thick.

Table 1). A Schenck AccuRate type MOD106M was used to feed microspheres into the extruder through a hopper (

Table 2). Once extruded, the foam was then water cooled and sent through a chopper where it became pelletized. Approximately 5-10 pounds of this pelletized syntactic foam was produced for each variant of thermoplastic syntactic foam. Panels for testing were molded using a plasticator to produce a molten charge and a Pasedena Hydralics Inc. hydraulic press to form 12"x12" panels approximately 6mm thick.

Table 1 Thermoplastic syntactic foams processed at MPAD facility showing microsphere content and resulting density. Foams are referred to by their sample/variant name in this thesis.

Sample/Variant	MB Density(g/cm^3)	Thermoplastic Resin	TP Density (g/cm^3)	V_f % Spheres	W_f% Spheres	W_f % Resin	Composite Density (g/cm^3)
PP-0	N/A	PP	0.95	0	0.00	100.00	0.950
PP-25	0.28	PP	0.95	25	8.94	91.06	0.783
PP-50	0.28	PP	0.95	50	22.76	77.24	0.615
TPX-0	N/A	4 Methyl Pentene	0.83	0	0.00	100.00	0.830
TPX-25	0.28	4 Methyl Pentene	0.83	25	10.10	89.90	0.693
TPX-50	0.28	4 Methyl Pentene	0.83	50	25.22	74.78	0.555

Table 2 Microsphere ID and compression properties

Microsphere	ID	Isostatic Collapse Pressure Min 80% Survival Level	
		Bar	PSI
Trelleborg	SID-311Z	379	5500

Thermoplastic polymers used were provided by BP (polypropylene grade 3541 impact copolymer) and Mitsui Chemicals (TPX grade TMM-25.) Pellets from each variant at different times during processing were sampled for burn-off testing to check microsphere content. Microspheres were dried before processing to prevent agglomeration in the hopper. Both of these polymers offer flexibility in processing for different manufacturing methods involving thermoplastics like extrusion and compression molding. Each polymer is low in density which reduces the weight penalty of the composite and adds unique energy absorbing features due to the viscoelastic nature of the polymer.

3.2. Experimental Methods

3.2.1. Vibration Analysis

Samples for vibration analysis were water-jet cut into 1" wide by 8" long beams by CMC Corporation. A Brüel & Kjaer (B&K) Type 8000 Impedance Head connected to a nylon stinger rod connected to a B&K Type 4809 Electrodynamic Shaker was used to support the sample in a free-free condition. Input force and output acceleration signals were fed to a B&K 2032 dual channel frequency analyzer through two Kistler Type 5004 dual mode pre-amplifiers.

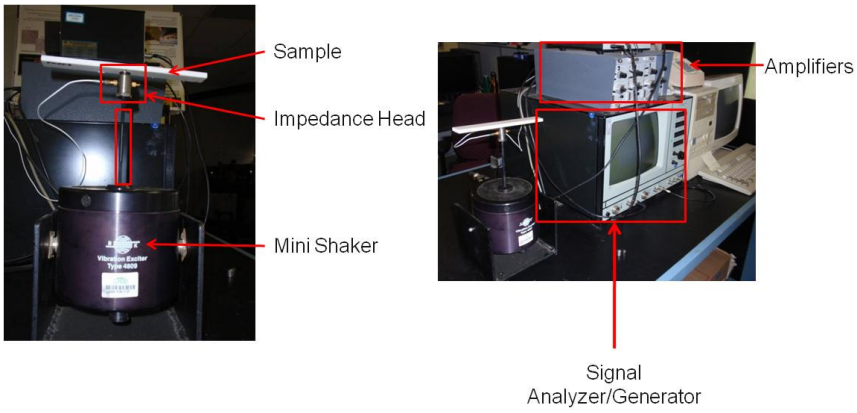

Figure 2 Vibration analysis setup showing sample, impedance head, stinger rod, mini shaker, pre-amplifiers, and frequency analyzer/generator

Using the generator a range of randomly generated frequencies amplified by a B&K Type 2706 Power Amplifier was used to excite the sample continuously in baseband mode. Figure 2 shows the experimental setup. The frequency response function (FRF) to the excitation was recorded and then exported to Microsoft Excel 2007 for further analysis. Resonance peaks of the samples response were measured and then examined closer by exciting those frequencies using a zoom mode. The damping ratio of the material was calculated by using the half-power bandwidth method shown in equation 2.

2

$$\zeta = \frac{f_2 - f_1}{2f_n}$$

Where ζ is the damping ratio of the material and f_1 and f_2 are their frequencies plus and minus 3dB in amplitude from the natural or resonance frequency, f_n. Damping is an important material characteristic of foams, especially for foams used for energy absorption. The amount of energy that the foam can absorb increases with increasing damping and could decrease the effect seen from blast or shockwaves.

3.2.2. Quasi-Static and Dynamic Compression

Samples were prepared using a CNC milling machine to precisely machine ½" diameter samples for quasi-static confined and unconfined compression, as well as dynamic high strain rate compression using the SHPB. Confined compression tests were conducted to understand the material behavior under hydrostatic conditions in order to better understand material properties and for comparison to unconfined compression. Under confined compression conditions it is easier to recognize the three regions of the stress- strain curve since the material is forced to crush uniaxially. Due to processing time and material availability, samples were all prepared using PP-50 TPSF for static and dynamic compression. A 5000 lbf Satec load frame was used to conduct all quasi-static compression tests. Two flat platforms, one swiveling platform and one fixed, were used to ensure as close to parallel compression of the samples. Figure 3 shows the compression setup used. For unconfined compression, the sample was simply placed between the two platforms.

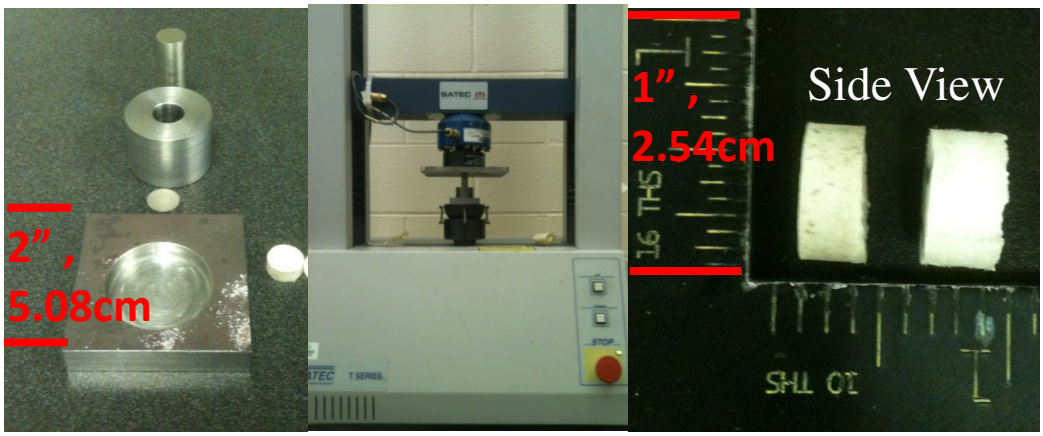

(A) **(B)** **(C)**

Figure 3 (A) Confined compression fixture (B) Confined compression fixture on load frame with leveling base and flat top platen (C) PP50 compressed sample on left, not compressed on right showing thickness difference

A Split Hopkinson Pressure Bar (SHPB) was used to conduct dynamic compression tests at high strain rates on PP50 foam samples. A striker bar was shot at different velocities at an incident bar which transmitted the stress wave through the sample and then to the transmitted bar. Since this particular SHPB was not yet fully instrumented a comparative study was done on the foam samples by their amount of damage or failure mode.

Figure 4 Split Hopkinson Bar setup showing barrel (1), incident (2), and transmitted bar (3)

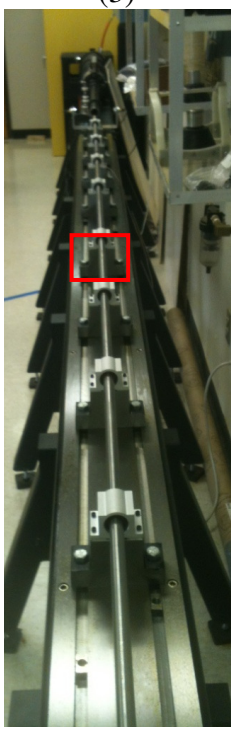

Figure 5 SHPB setup with sample location outlined in red

3.2.3. Low Velocity Impact

Approximately 3”x 3” (7.62cm x 7.62cm) panels were prepared for testing. These panels consisted of a 6mm thick compression molded syntactic foam back bonded to a 2mm thick panel of Tegris using 3M VHB Tape. An instrumented Instron Type 8250 drop weight impact testing machine using a half inch hemispherical tup with Dynatup 930I data acquisition system was used to conduct LVI by varying the drop height and using a constant mass of 11.13 kg. Both load and force versus time curves were obtained from the individual tests. A ½” (1.27cm) hemispherical impactor made of hardened steel was used for impact to the 3”x3” under unclamped conditions. A Tegris panel bonded to a TPX25 foam panel would provide desirable properties for both automotive and other applications needing light weight panels. The Tegris facesheet is able to capture impact loads with its 0-90 ply construction containing many strong fibers, while the TPX25 foam back panel would be capable of dissipating the impact energy throughout the viscoelastic matrix and voids introduced by the glass microspheres. These types of panels could assume applications such as automotive paneling for interior or exterior use and others alike.

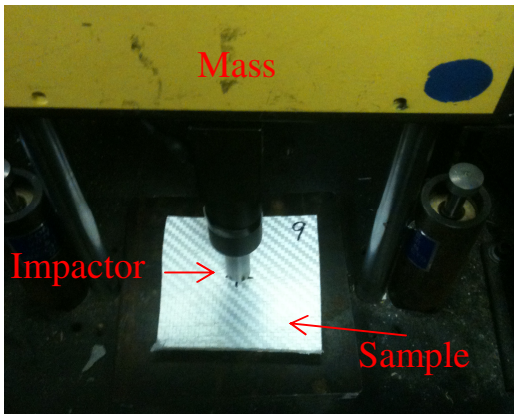

Figure 6 Low velocity impact setup showing the mass, impactor, and sample location/orientation (Tegris face up)

3.2.4. Ultrasonic Testing

Beams mentioned in Section 3.2.1 were used for through transmission testing using two dry coupling WD50-2 2MHz transducers. Readings were taken from a Tektronix TDS210 Digital Real-Time Oscilloscope and recorded into Microsoft Excel2007. A Panametrics 5800 computer controlled pulser and receiver was supplied the signal to the transducers. In addition a 6"x6" panel was prepared from each of the four TPSF variants to conduct ultrasonic c-scans. Using the time of flight through the material modulus can be estimated since time of flight changes in different materials due to more or less attenuation of the signal by the material. The velocity, or speed of sound through the material, is calculated by:

3

$$V = \frac{thickness}{time\ of\ flight}$$

Using ultrasonic transducers it is possible to also calculate Poisson's ratio. By placing the transducers appropriately a longitudinal and transverse velocity can be calculated. From this Poisson's ratio can be calculated using the following:

4

$$\nu = \frac{1 - 2\left(V_t/V_L\right)^2}{2 - 2\left(V_t/V_L\right)^2}$$

Then Young's modulus can be calculated using Poisson's ratio and the density of the material by:

$$E = \frac{V_L^2 \rho (1+\nu)(1-2\nu)}{1-\nu}$$

From these calculations moduli from other test methods could be compared.

3.2.5. Modeling

LS-DYNA, Hypermesh, and PTC CREO were used to run static and dynamic compression simulations for a 25% by volume fraction of glass microspheres for one unit cell consisting of one glass microsphere and the surrounding matrix. Details for the modeling are found later in Section 4.4.

In summary, the following table shows material types and testing along with the rationale for the chosen test method. There are many different potential applications for TPSF. PP50 was chosen for the compression tests because it would have the largest stress plateau due to its high microsphere content making it easier to make a comparison across the board to the same material for high strain rate testing. Since TPX has the lower density of the two polymers it was chosen for the low velocity impacts to further reduce weight penalty in possible important applications such as military infantry helmet liners.

Table 3 Test methods listed with the material system used followed by the desired parameter to be measured or compared and the rationale behind the testing

Test	Material System	Parameters Tested	Rationale
Burn-off	ALL	Microsphere content	Check target density after processing
Ultrasonics	ALL	Microsphere distribution	Check distribution after processing panels
Vibration Analysis	ALL	Damping Ratio	Comparison of TPSF to conventional materials used for damping
Quasi-Static Compression	PP50	Uniaxial compression strength	Strain rate sensitivity and definition of 3 characteristic regions
Dynamic Compression	PP50	Uniaxial high strain rate compression strength	Strain rate sensitivity comparison to quasi-static and reaction to high strain rate conditions
Low Velocity Impact	TPX25	Reaction to blunt low speed impact	Simulation of possible application

4. RESULTS AND DISCUSSION

4.1. Processing and Production Analysis

4.1.1. Burn-Off Measurements

After processing, the first steps taken towards testing were to validate the production method to check if target densities were met. Samples of approximately 10 grams were place into aluminum trays and weighed. Samples were then placed in a burn-off oven at 500°C for 1 hour. Samples were checked after 1 hour to make sure that all polymer had burned away leaving only the glass microspheres. Trays were then weighed again to check the weight fraction of microspheres against the values listed in Table 2.

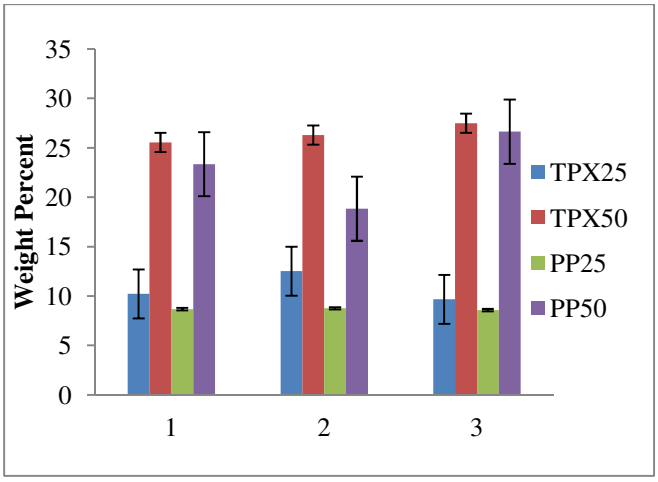

Figure 7 The standard deviation in microsphere content after burn off between 3 samples of each TPSF taken at different processing times directly from the extrusion line

Figure 7 shows samples densities are within one standard deviation of the mean for each of the samples tested for the same type of TPSF. This indicates that microspheres were

properly distributed into the polymer during the extrusion process. Further testing was done to check microsphere content and distribution in the next section.

4.1.2. Ultrasonic Inspection

Ultrasonic inspection was a NDT method chosen to check microsphere distribution. As mentioned earlier an ultrasonic C-scan was conducted using 6”x6” panels from 12”x12” compression molded panels.

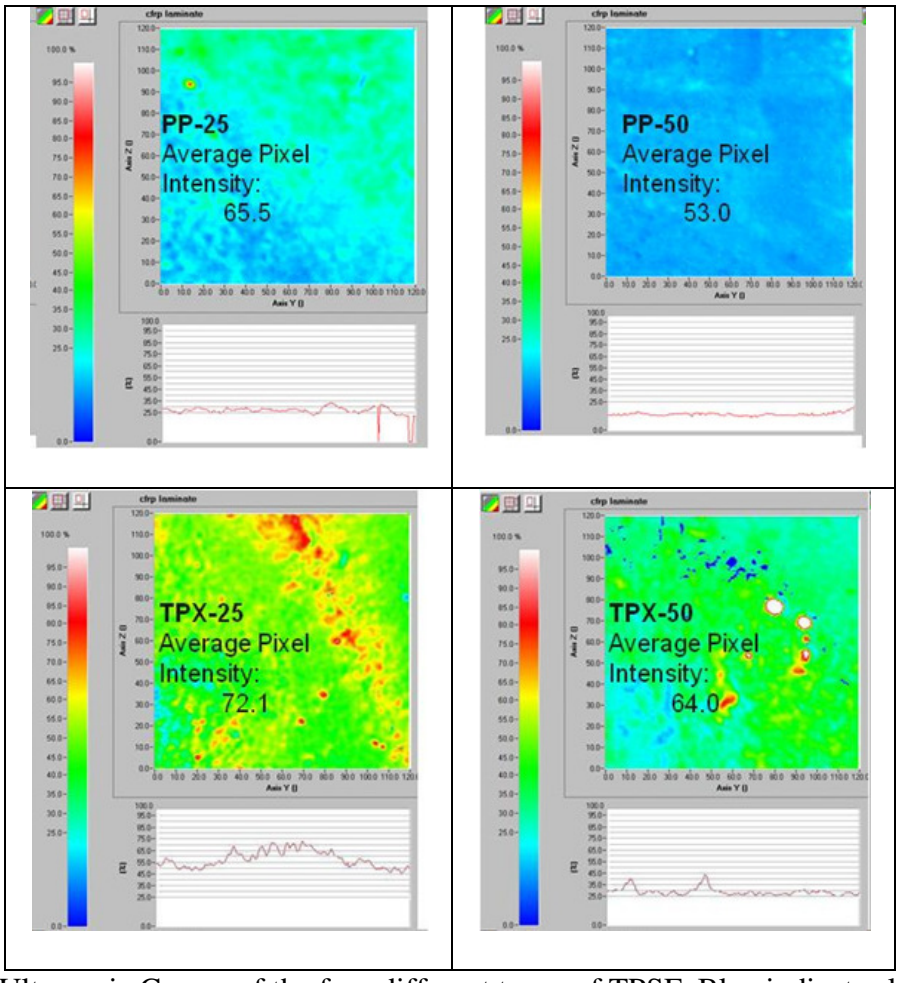

Figure 8 Ultrasonic C-scan of the four different types of TPSF. Blue indicates low attenuation relative to average pixel intensity. White or red indicates high attenuation relative to average pixel intensity. This indicates that higher attenuation is seen in the TPX samples.

Higher attenuation is seen in the TPX samples than in the PP samples. From the C-scan it is apparent that the lower volume fraction of glass microspheres in the foam show better results in microsphere distribution. This type of problem is most likely from the plastication stage of processing where extruded pellets are fed to a single screw plasticator which compounds and melts the foam pellets to form a molten charge. Some pellets may not have fully melted causing local agglomerations in the panel.

After vibration analysis, each foam beam was point scanned with ultrasonic transducers by hand. This was to ensure there were no defects in the beam that would cause phase shifts or inaccurate damping measurements from the frequency response function. Results can be seen in Section 4.2.

4.2. Vibration Analysis

As mentioned in section 3.2.1 TPSF beams were excited continuously under a free-free boundary condition as shown in Figure 2. The FRF for three beams of each TPSF variant was plotted and averaged. The averages were then plotted against each other for direct comparison of their baseband FRF. Figure 9 shows the comparison of baseband FRF on average for each different type of TPSF. The PP25 foam shows a frequency shift away from the rest of the foams indicating more damping. The damping ratios were calculated and plotted for each of the peaks seen in Figure 9 for each of the 12 total beam samples. The results can be seen in Figure 10. The frequency shift mentioned above indicated that the PP25 TPSF was better at damping the vibrations across the baseband of frequencies showing a 15-20% shift in frequency. It can be seen that the damping ratio of the PP25 samples is higher than the other TPSF until the higher frequency region where it becomes unclear which TPSF is performing better due to the fluctuation in data. The

damping ratio for PP25 is as much as nine fold higher in some instances than a baseline of aluminum. At 5000 Hz, the damping ratio for PP25 is 0.047 compared to aluminum at 0.005. Neat PP quickly attenuates low frequencies but does not aid in damping in the higher frequency ranges with a damping ratio near 0.08 near the 4000 Hz range.

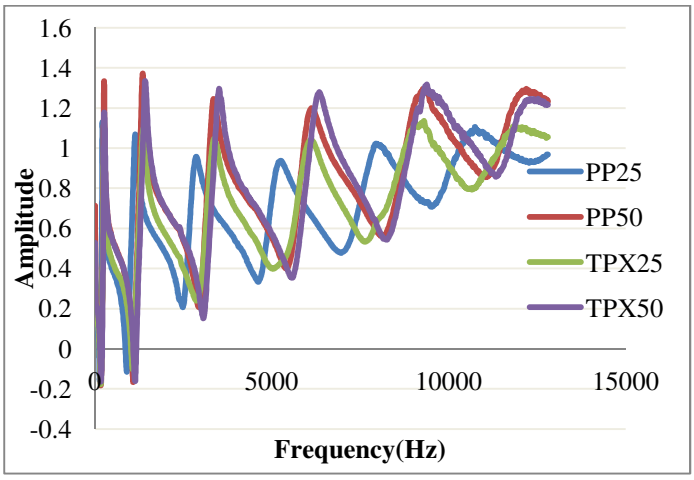

Figure 9 Baseband comparison of 1"x8" beams normalized to weight showing a 15-20% shift in frequency by PP25 samples

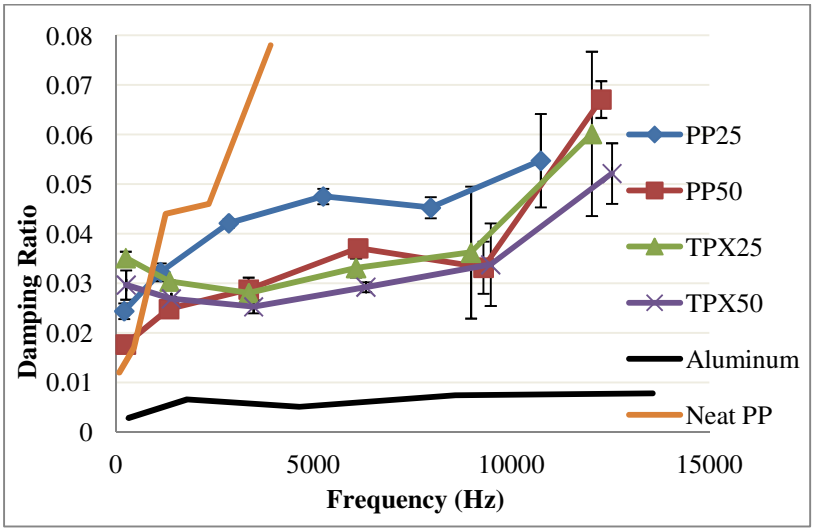

Figure 10 Damping ratio comparison for TPSF's, neat PP, and Aluminum with error bars indicating one standard deviation

As a result of the FRF of the TPSF's and their corresponding damping ratios, the PP25 samples were further investigated because of their superior performance when compared

to the other foams. An ultrasonic point scan was used with two transducers for through transmission and the time of flight was recorded at every ½" interval along the length of the beam.

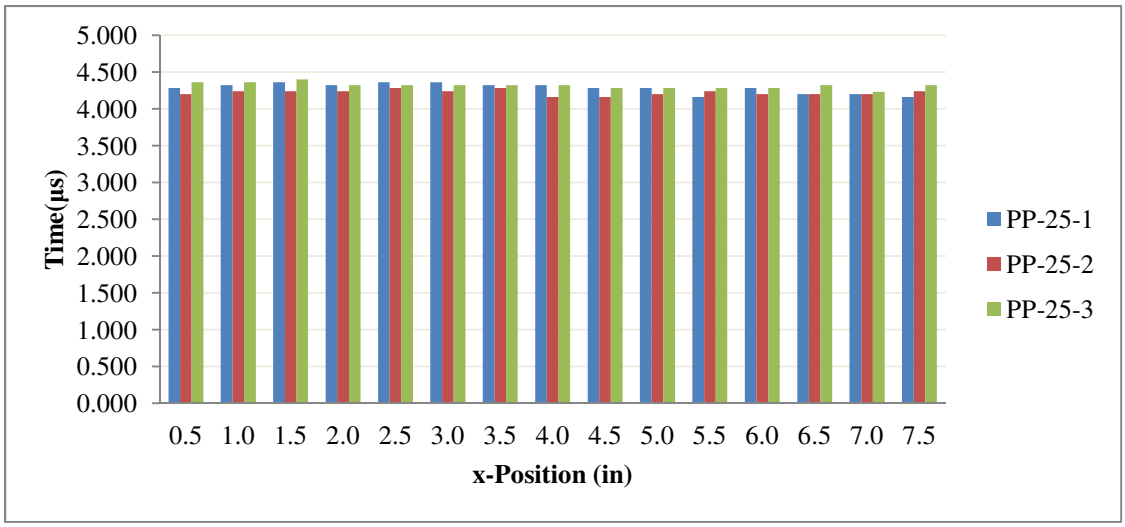

Figure 11 Ultrasonic point inspection using through transmission and recording time of flight along the length of each of the three 8" PP25 beams

Time of flight through the beam samples did not vary significantly as all samples averaged just over 4 micro seconds. Other factors that affect the FRF during vibration analysis, besides defects, can be linked to weight and thickness of the samples. Geometry was not an issue since all samples were precisely water jet cut. Table 4 shows the rest of the measurements taken from the TPSF beam samples to help verify that the PP25 variant is performing better for reasons other than factors like weight, thickness, or density. Target density was most closely related to the PP25 samples seen in Table 4. However the weight of the PP25 beams is slightly higher than the rest possibly giving more inertial resistance to the excitation from the analysis. The weight of the beams may be causing the frequency shift seen in Figure 9.

Table 4 Eight foam beam specimen with their individual densities, target density based on processing parameters, percent error from each set of 3 beams of the same variant, average thickness of each beam, and individual weights are shown

BeamID	Density g/cm^3	Target Density	Average %Error	Average Thickness (mm)	Weight (g)
PP25_1	0.787	0.783	1.13	6.66	26.9
PP25_2	0.788	0.783		6.58	26.6
PP25_3	0.800	0.783		6.68	27.4
PP50_1	0.669	0.615	8.72	6.71	23.0
PP50_2	0.673	0.615		6.63	22.9
PP50_3	0.664	0.615		6.87	23.4
TPX25_1	0.750	0.693	6.48	6.86	26.4
TPX25_2	0.730	0.693		6.94	26.0
TPX25_3	0.733	0.693		7.26	27.3
TPX50_1	0.682	0.555	22.67	6.77	23.7
TPX50_2	0.683	0.555		6.62	23.2
TPX50_3	0.677	0.555		6.71	23.3

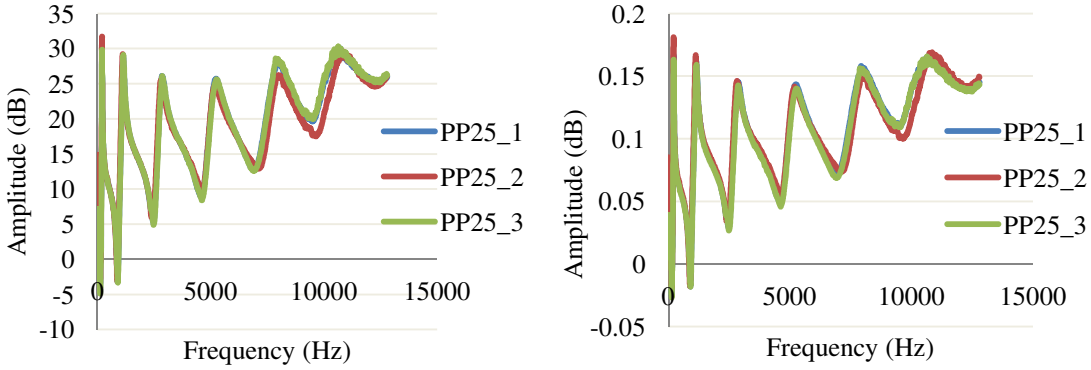

(A) **(B)**

Figure 12 (A) FRF of PP25 samples without normalization (B) FRF of PP25 samples normalized to thickness

From Figure 12 it is shown that thickness does not affect the FRF between samples. All PP25 samples show similar responses to the continuous vibrations.

4.3. Quasi-Static Compression, Dynamic Compression, and Low Velocity Impact

As mentioned in Section 1.2.2, the most common mode of deformation for foams is under compression. Quasi-static compression testing has been adopted for this study.

Both a confined and unconfined compression setup was used. Tests were run at two different rates using a total of three samples for each rate and each type of compression setup. It is recognized that these experiments do not represent true stress or strain conditions. As mentioned by Gupta et al. [17], the stress tensor for uniaxial stress can be divided into two separate components, hydrostatic and deviatoric. The hydrostatic stress is responsible for the compressive stress in the test specimen while the deviatoric contributes to the shear stress seen in the material. The stress tensor is represented by the following:

6

$$\sigma_{ij} = \begin{bmatrix} -\sigma & 0 & 0 \\ 0 & 0 & 0 \\ 0 & 0 & 0 \end{bmatrix}$$

where σ is the applied compressive stress and σ_{ij} is,

7

$$\sigma_{ij} = \sigma_{hyd} + \sigma_{dev}$$

where the hydrostatic and deviatoric stress are represented by,

8

$$\sigma_{hyd} = \begin{bmatrix} \frac{-\sigma}{3} & 0 & 0 \\ 0 & \frac{-\sigma}{3} & 0 \\ 0 & 0 & \frac{-\sigma}{3} \end{bmatrix}$$

9

$$\sigma_{dev} = \begin{bmatrix} \frac{-2\sigma}{3} & 0 & 0 \\ 0 & \frac{\sigma}{3} & 0 \\ 0 & 0 & \frac{\sigma}{3} \end{bmatrix}$$

The hydrostatic portion of the stress produces only elastic deformation while the deviatoric contributes to plastic deformation of the test specimen [17]. Thus it is important to consider the elastic section of the stress-strain curve before plastic deformation and shear stress dominate in the unconfined compression setup.

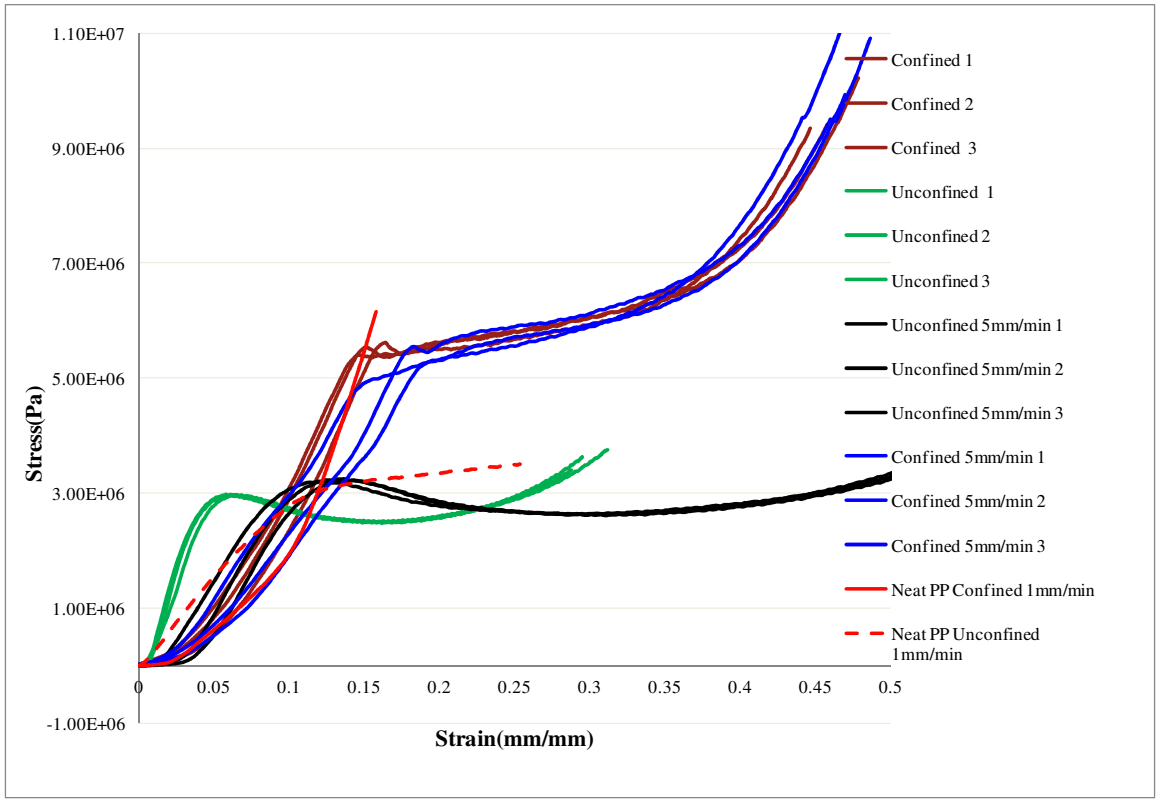

Figure 13 Compilation of quasi-static compression tests under confined and unconfined conditions at different compression rates

Figure 13 shows 14 quasi-static compression tests done for the PP50 batch of foams only. The dynamic tests were conducted on only one variant of the TPSF- the PP50 samples. This approach was adopted to systematically study the compression response across a range of confined and unconfined conditions. The PP50 foams exhibit typical behavior under quasi-static compression with a yield stress of approximately 6 MPa and 3 MPa under unconfined conditions, both showing stress plateaus. In the confined compression the shearing effect is significantly reduced resulting in almost pure uniaxial compression.

In the unconfined tests however, after some elastic deformation samples began to expand and barrel outwards eventually thinning significantly. This causes the stress plateau to look longer than it actually is since the area of the sample is increasing; the stress is decreasing close to the same rate causing what looks to be an extended plateau. At the compression rate of 1mm/min the neat PP and PP50 foam show similar yield strengths under unconfined conditions. On the other hand, when neat PP is compressed in the confined fixture stress increases slower than in the foam but then surpasses the foam in peak stress. Barreling was the only noticeable failure of the unconfined compressed foam samples and in the neat PP.

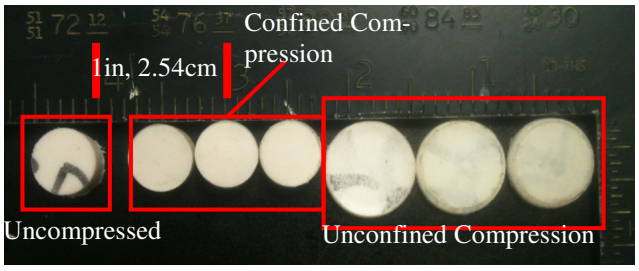

Figure 14 Uncompressed sample, confined compression samples, and unconfined compression samples side by side showing compression orientation

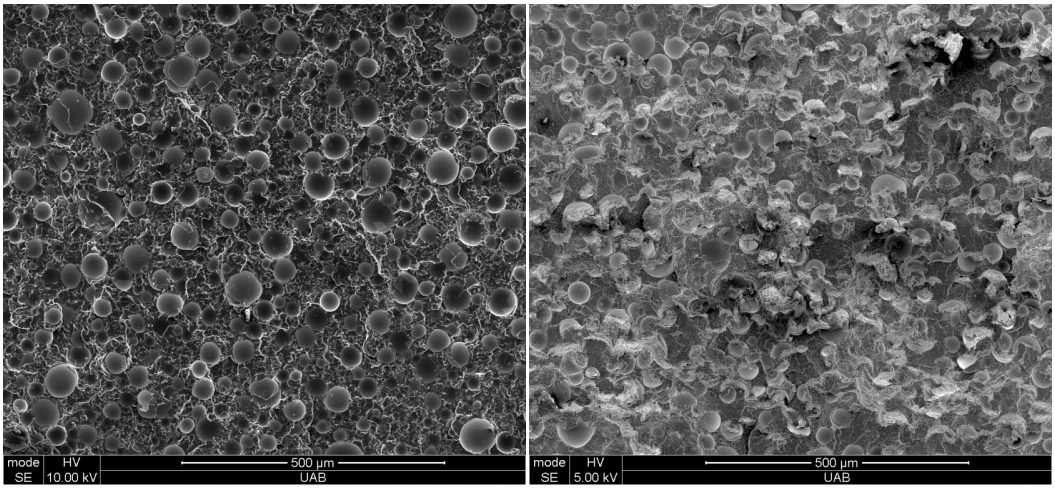

(A) **(B)**

Figure 15 SEM micrographs side by side of a fracture surface from a confined compression sample (A) before compression showing whole microspheres on the surface and (B) after compression showing almost all broken microspheres on fracture surface

SEM micrographs show that the microspheres have been shattered after confined compression. Samples were put in liquid nitrogen to cool and were then fractured to show the compressed and uncompressed surfaces.

Dynamic compression tests showed different failure modes than quasi-static compression. As expected the material was rate sensitive and failed in different modes with increasing strain rate. During quasi-static compression, samples began to barrel and flatten after a section of elastic deformation. Results from dynamic compression were similar at lower strain rates on the SHPB. However, with increasing strain rate different failure features formed from the induced stress wave. Since the SHPB was not fully instrumented at the time of testing it was decided to show a comparative study showing the effect of increasing strain rate on the PP50 foam samples.

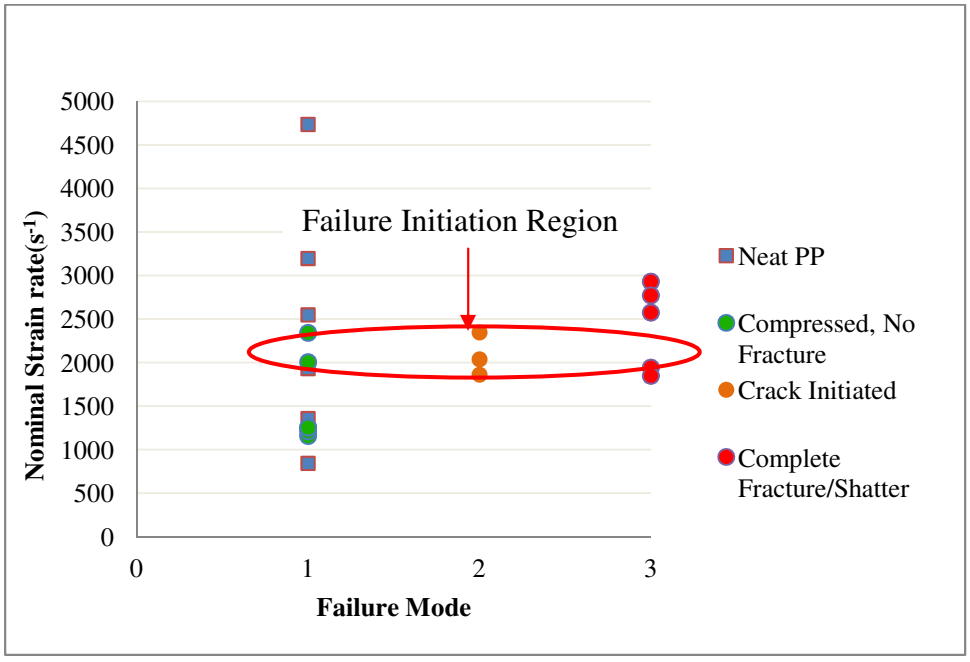

Figure 16 SHPB tests done on neat PP and PP50 foam sample with color corresponding failure modes. Neat PP did not fracture or shatter during any test

Strain rates in Figure 16 do not represent the actual strain rate since the Split Hopkinson Bar was not instrumented for these tests. Using the conservation of momentum strain rate was calculated purely based on velocity of the striker bar and the thickness of the sample. A failure trend was noticed beginning around 2200s^{-1}. As strain rate increased samples were compressed, then at higher strain rates formed cracks, and even higher strain rates caused shattering of the sample usually with the back face remaining intact. The data in Figure 16 provides the trends of high strain rate failure of these samples. The strain rate does significantly affect the failure mode of the syntactic foam. The strain rate effect on the neat PP is unclear without instrumentation since there are no samples cracked or shattered. Change in thickness seemed to take a linear path with increasing strain rate.

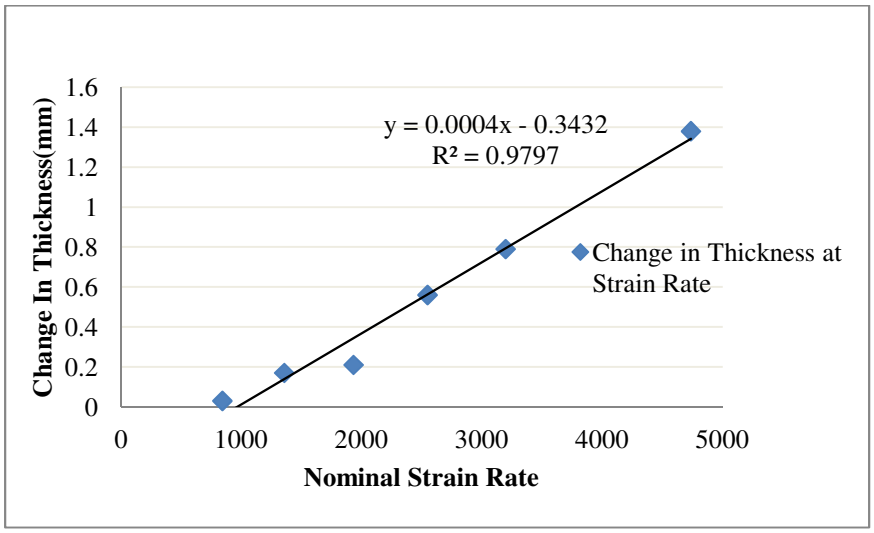

Figure 17 Comparison of change in thickness of neat PP samples over increasing strain rates

In order to make some comparison change in thickness was plotted against strain rate for neat PP samples. With increasing strain rate, neat PP samples followed a linear path when comparing change in thickness. Normalizing the data to thickness did not significantly

affect results. Some images were taken after testing to show the described failures in Figure 16. They are shown in Figure 18. Three distinct failure modes were apparent after the completion of testing. First, samples remained intact and in a compressed state as shown below with increase in diameter and decrease in thickness. Next, at slightly higher strain rates samples began to crack indicating strain rate had begun to affect the viscoelastic nature of the polymer. Polymer chains have less time to stretch and begin to break causing fracture in the material due to discontinuity caused by the glass microspheres. At even higher strain rates brittle catastrophic failure occurs and the sample shatters, cracking along paths of microspheres. The inclusion of glass microspheres at high strain rates decreases the length a crack has to travel to reach the next microsphere causing the brittle failure seen below.

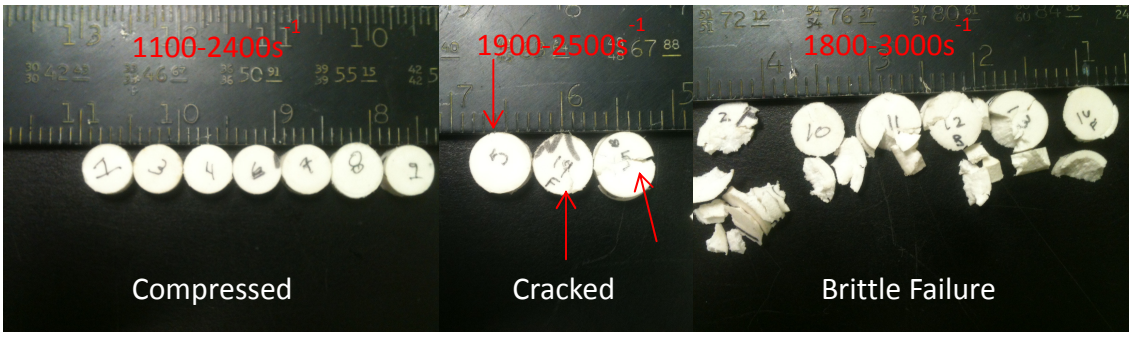

Figure 18 HSR samples after impact pictures showing crack formation, crush, and shatter

LVI testing showed the resilience of the syntactic foam to repeated and single impacts. Drop heights for the falling weight of 11kg mass ranged from 0.25 to 1.15m drop height. Some tests involved repeated impact while others were only a single impact. One of the key applications of the work is for blast resistant helmet liners, where weight reduction is critical. Compared to the PP resin, the TPX resin has lower density; hence the TPX system was considered in the single and repeated impact tests. TPX25 samples

were bonded to a Tegris face sheet to simulate a similar situation that this foam could see in practical applications. Since both of these materials are lightweight and consist of thermoplastic constituents, processing and production of such parts for applications such as the helmet liner would require the least amount of processing steps. The Tegris and TPX25 foam offer a pairing that can both blunt or capture impact energy and then dissipate in the TPSF composite. According to Milliken & Company, Tegris is a 100% polypropylene composite with excellent impact resistance, lightweight, and stiffness. This makes it an ideal facesheet for energy absorbing foam like the TPSF in this study as weight is not compromised and impact resistance is improved.

As a baseline, one TPX25 panel and one Tegris sheet were placed under the impactor and tested separately.

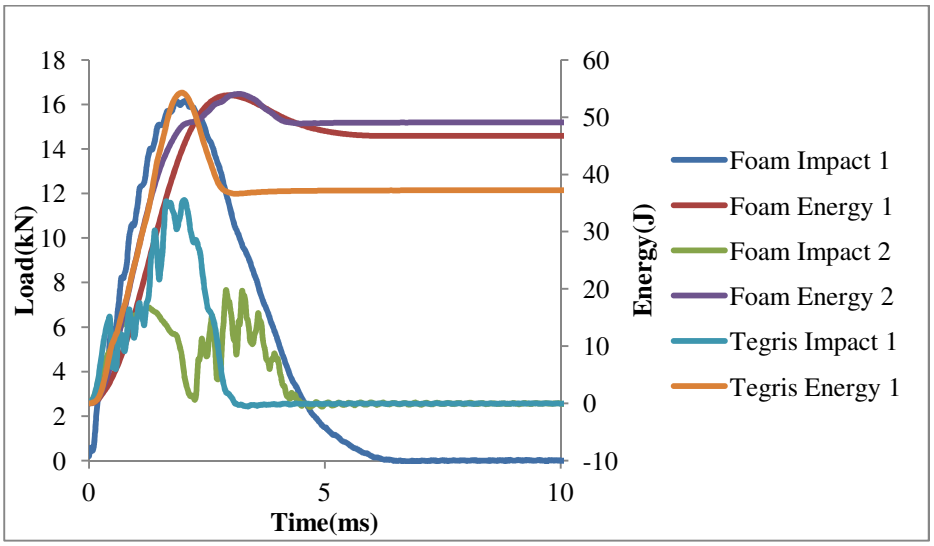

Figure 19 Load and energy curves for TPX25 foam and Tegris face sheet tested separately from a 50cm drop height. Each impact in the key represents the load seen by the sample while the energy is represented on the second axis. Each sample was struck under unclamped condition with steel backing until failure. Foam impact 2 indicates two peaks in load, the foam panel crushing and then puncturing due to impact and striking the steel backer.

The foam panel took two hits at 50J before fracturing upon the second impact and the thin Tegris face sheet failed after the first impact at 50J. With the inclusion of glass microspheres in the foam, the first impact causes local damage. When the second impact strikes the same location the energy is too great for the already damaged panel and caused the panel to fracture catastrophically. After this initial test several panels were impacted at various drop heights trying to find the maximum drop height that would not result in catastrophic failure.

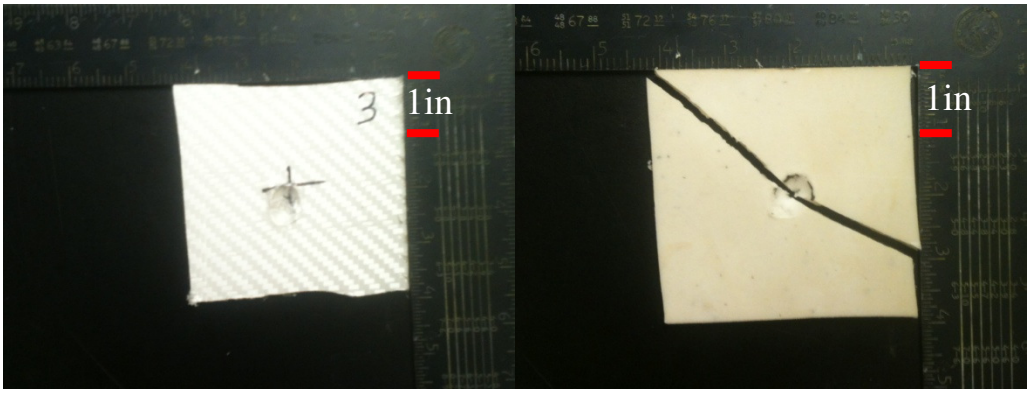

Figure 20 Tegris sheet on left punctured, TPX25 Panel on right showing brittle failure

In addition, because of the intended application of the TPSF's for protection applications, a low drop height was chosen of 0.25 m to conduct a multiple impact test. This panel was subject to 25 impacts on the same area. No catastrophic damage occurred. The first 6 impacts recorded are shown in Figure 22.

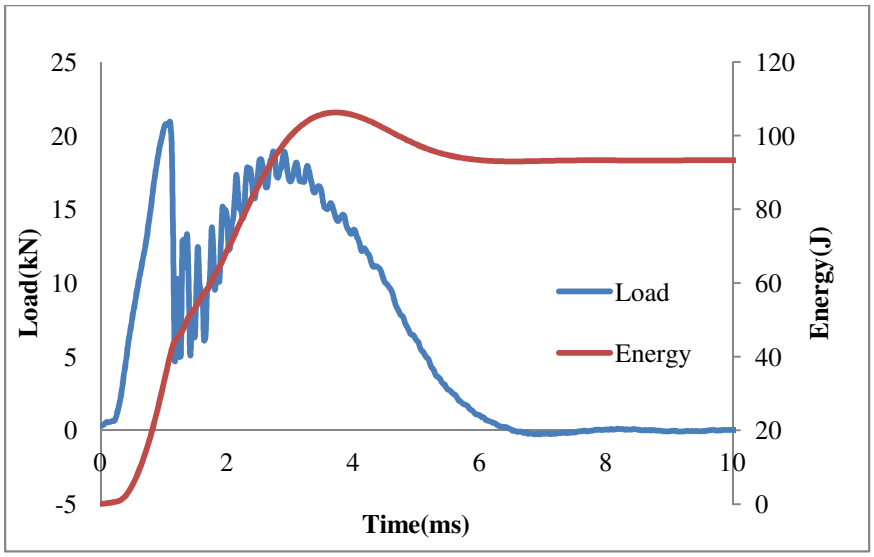

Figure 21 Maximum impact sustained by TPX25-Tegris panel without catastrophic failure

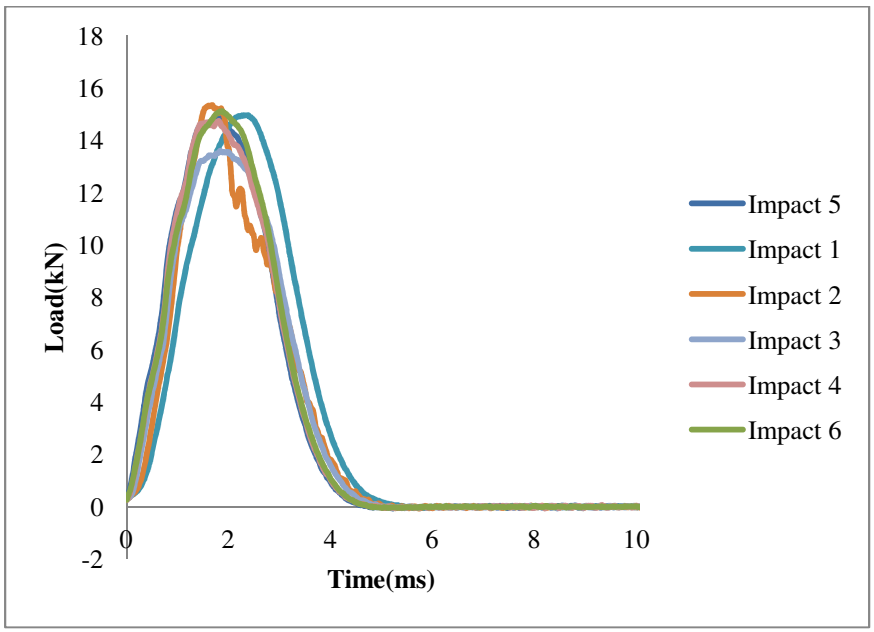

Figure 22 Successive impacts from 25 cm drop height with 11kg mass

After repeated impacts the TPX25-Tegris panel had minimal indentation as the only visible damage upon inspection.

Figure 23 Panels impacted from various drop heights. Front Tegris face sheets are shown in the top row with corresponding back faces shown in the bottom row each panel was subjected to a different loading varied by drop height included in Table 4.

Drop heights for the panels are listed in Table 5. Panels 2 and 8 were discarded because they fractured along a portion of unmelted foam pellets in the panel causing early failure of the specimen. No penetration of sample means there was no backface penetration. Penetration denotes full puncture of Tegris facesheet and foam backer. Brittle failure refers to the specimen that shattered in a brittle manner as a result of impact.

Table 5 Drop heights for constant mass LVI tests TPX25/Tegris specimen

	Thickness (mm)	Drop Height(cm)	No Penetration	Penetrate	Brittle Failure
1	11.84	60	x		
2	11.61	80	x		
3	10.92	50			
4	11.56	90	x		
5	11.35	25	x		
6	11.07	50			x
7	11.48	115			x
8	11.25	100		x	
9	11.86	70	x		

With varying drop height the panels' reaction to the impact load was recorded in Table 5. From the results it was found that the combination of Tegris and TPX25 offer an alternative for lightweight paneling for automotive and other applications where energy absorption is important. These panels were successful in withstanding high impact loads from a blunt object as well as repeated impact. In addition TPSF like PP50 showed the

importance of strain rate and the materials rate sensitivity when considering this material for high strain rate applications. Different failure modes were seen with increasing strain rates in contrast to the quasi-static testing. Quasi-static compression did show signs of strain rate sensitivity that was noticeable in their stress strain curve in contrast to the high strain rate specimen failures shown in Figure 18.

4.4. Modeling

As mentioned in Section 1.2.4, there has not been much modeling done for syntactic foams. In addition most modeling has been done in the static region. Since this particular study considers materials that would see a range of impacts, a dynamic model approach would be helpful. In that respect, matrix strain rate sensitivity could be studied along with the interaction of the HGMS and the surrounding matrix in order to develop a model to fully understand the behavior of TPSF. The general approach to this simulation started with the generation of a simple geometry. One representative unit cell of thermoplastic syntactic foam was modeled in PTC Creo Parametric. The unit cell consisted of one glass microsphere and the surrounding thermoplastic matrix with a wall thickness of 1 micron show in Figure 24. The model was generated in this manner for ease of changing volume fractions of glass microspheres in latter simulations.

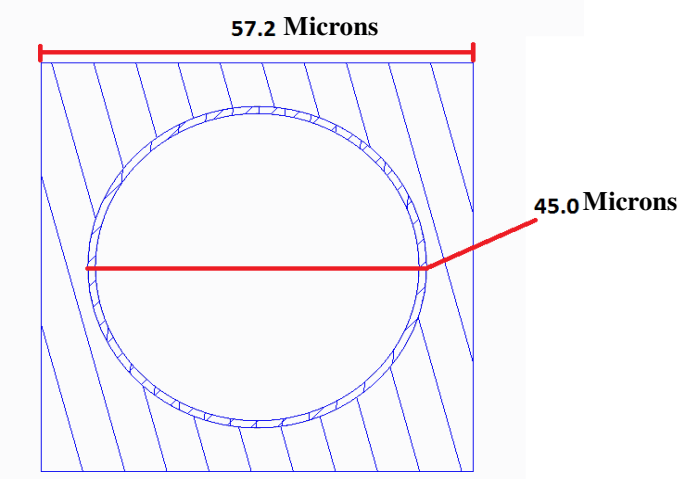

Figure 24 Cross section view of 25% volume fraction glass microsphere syntactic foam with a 1 micron wall thickness

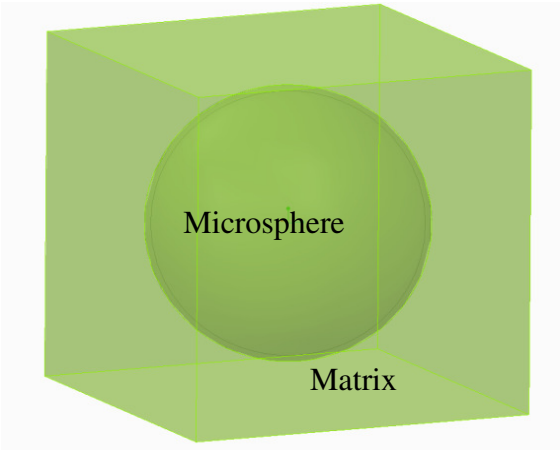

Figure 25 3-D representation of unit cell used for dynamic and static simulation showing the microsphere within the matrix

Using Hypermesh meshing program, a 3D mesh was generated for analysis. Both the glass microsphere and matrix were meshed with tetra elements and approximately 47,000 elements were created. Coarser meshes were created but resulted in negative volume failures during simulation.

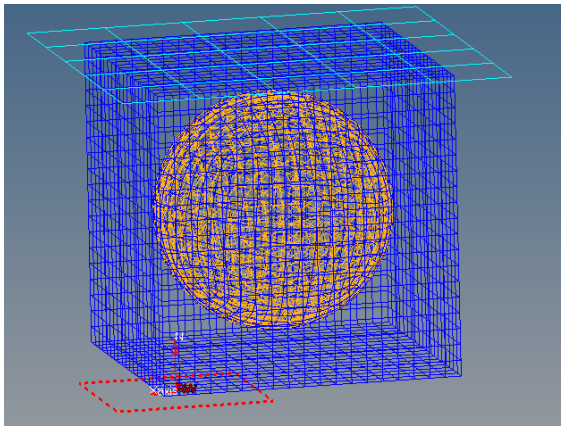

Figure 26 Mesh generated for unit cell of syntactic foam showing moving boundary wall (top), foam (matrix and microsphere mesh), and rigid wall (bottom)

Once the mesh was generated materials, properties, initial and boundary conditions were created. A rigid wall was used to constrain the bottom surface of the cell. PRESCRIBED_BOUNDARY_MOTION was assigned to a rigid body to which controlled velocity and displacement of the impactor. MAT_RIGID was assigned properties of steel to imitate a compression test setup. Contact interfaces were setup between the surface of the sphere and the matrix as well as the matrix to the impactor. An intermediate velocity of 1mm/ms was assigned to the rigid plate for duration of 35ms. This time was sufficient to allow for full cell collapse.

The glass microsphere was modeled using MAT6, a viscoelastic model, using properties of glass. Solid elements were used. Other considerations for future models include MAT110, the Johnson Holmquist ceramics model. Due to the complexity of this model and time constraints it was not used but would be a better option for future testing. This material model required data that was not attainable without an instrumented SHPB. That data would have been needed to investigate strain rate effects in the model.

The thermoplastic matrix was modeled with material model 3. MAT 24 will be employed in later models to show rate effects but for computational efficiency MAT3

was better to generate a working model. Solid elements were used in the mesh generation.

For analysis, several simulations were run showing the compression of the microsphere, the matrix, and then the unit cell containing both. Refer to Figure 24 for dimensional references.

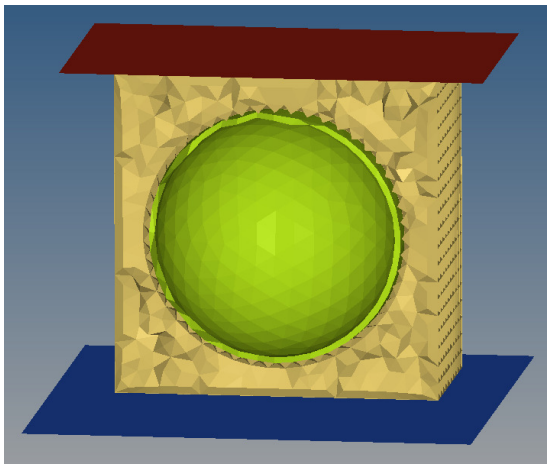

Figure 27 Snapshot of cross section with 3-d solid elements, moving rigid boundary wall (red), matrix elements (beige), microsphere elements (yellow), confined rigid wall (blue)

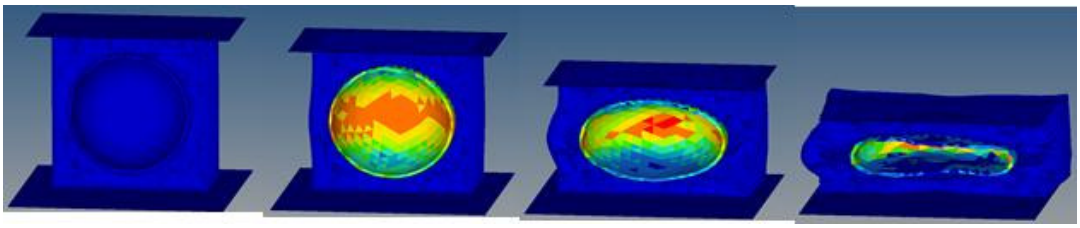

Figure 28 LS-DYNA simulation crush sequence during compression simulation showing equivalent stress, areas of red show higher equivalent stress than blue

Rate sensitive material models are available in LS-DYNA. However, testing limitations made it unreliable to model further and come closer to validation. The stress values obtained for this particular simulation did not accurately represent the TPSF. Further testing and modeling would be required to accurately simulate the TPSF.

5. CONCLUSIONS

Several adaptations were made in this study to conserve the number of experiments and material used. Each test was conducted to showcase the ability of the TPSF to adapt to different applications and in turn their response under specific testing conditions. Vibration, ultrasonic, and burn-off testing were conducted across all TPSF variants for a broad comparison of damping capabilities and processability. Quasi-static and high strain rate testing used the same material variant, PP50, to compare across the board strain rate sensitivity under uniaxial compression conditions. Tegris and TPX25 panels were used for low velocity impact testing because of their low weight penalty and ability to dissipate impact energy.

1) Burn-off tests and ultrasonic data show that polypropylene foams showed better microsphere distribution. Target densities were closer to actual density. TPX samples showed more attenuation in the C-scans.
2) Vibration analysis showed TPSF have better damping characteristics than other commonly used materials like neat polypropylene and aluminum. The PP25 showed the most improvement in damping capabilities compared to the other TPSF's.
3) Quasi-static compression tests did not show strain rate sensitivity. However, PP50 foams displayed characteristic behavior of foam under uniaxial compression showing the typical stress-strain curve. When compared to neat PP it can be seen that the amount of energy absorbed by the PP50 foam would be much higher.

Confined compression tests showed higher yield strength since shearing could not occur and cause barreling like in the unconfined specimen.

4) High strain rate tests did show a strain rate dependence based observation of failure modes. At strain rates close to 2300s^{-1} samples compressed similarly to the quasi-static tests, experiencing some barreling and reduction in thickness. They also showed edge cracking and sometimes complete brittle failure, shattering into multiple pieces.
5) LVI testing was conducted with constant mass and varying drop heights. Test heights ranged from 25 to 115cm. PP50-Tegris panels survived impact energies as high as 108J. Repeated impacts at 25cm drop height did not produce significant damage after 25 impacts.
6) LS-DYNA modeling approach shows possibilities of creating a dynamic model that could be verified by testing once more information is gathered for the rate dependence of the syntactic foam. Strain rate material models could be employed as well as interfacial strength between the glass microsphere and the surrounding matrix.

6. REFERENCES

[1] H. Klaus, O. Huber, G. Kuhn, ADVANCED ENGINEERING MATERIALS 7 (2005) 1117-1124.
[2] E. Rizzi, E. Papa, A. Corigliano, International Journal of Solids and Structures 37 (2000) 5773-5794.
[3] N. Gupta, V.C. Shunmugasamy, Materials Science and Engineering A 528 (2011) 7596-7605.
[4] G.M. Gladysz, K.K. Chawla, Journal of Materials Science 41 (2006) 3959-3960.
[5] U.K. Vaidya, S. Pillay, S. Bartus, C.A. Ulven, D.T. Grow, B. Mathew, Materials Science and Engineering: A 428 (2006) 59-66.
[6] E. Woldesenbet, S. Peter, Journal of Materials Science 44 (2008) 1551-1559.
[7] C.S. Karthikeyan, C.R.L. Murthy, S. Sankaran, Kishore, Bulletin of Materials Science 22 (1999) 811-815.
[8] G. Li, V. Muthyala, Composites Science and Technology 68 (2008) 2078-2084.
[9] R.F. Gibson, Journal of Materials Engineering and Performance 1 (1992) 11-20.
[10] R.D. Adams, M.R. Maheri, Damping in advanced polymer-matrix composites, in: Proceedings of the International Symposium on High Damping Materials 2002, August 22, 2002 - August 24, 2002, vol 355, Elsevier Ltd, Tokyo, Japan, 2003, pp. 126-130.
[11] A.C.F. Chen, H.L. Williams, Journal of Applied Polymer Science 20 (1976) 3403-3423.
[12] B. Song, W. Chen, D.J. Frew, Journal of Composite Materials 38 (2004) 915-936.
[13] N. Gupta, Materials Letters 61 (2007) 979-982.
[14] N. Gupta, Journal of Composite Materials 39 (2005) 2197-2212.
[15] N. Gupta, Characterization of syntactic foams and their sandwich composites modeling and experimental approaches, in: Louisiana State University, Baton Rouge, La., 2003.
[16] N. Gupta, Materials letters. 61 (2007) 979.
[17] N. Gupta, Kishore, E. Woldesenbet, S. Sankaran, Journal of Materials Science 36 (2001) 4485-4491.
[18] N. Gupta, E. Woldesenbet, Journal of Composite Materials 39 (2005) 2197-2212.
[19] N. Gupta, E. Woldesenbet, Kishore, Journal of Materials Science 37 (2002) 3199-3209.
[20] E. Woldesenbet, N. Gupta, A. Jadhav, Journal of Materials Science 40 (2005) 4009-4017.
[21] E. Woldesenbet, P. Mylavarapu, Strain 47 (2011) 29-36.
[22] E. Woldesenbet, S. Peter, Journal of Materials Science 44 (2008) 1528-1539.

[23] F. Grosjean, N. Bouchonneau, D. Choqueuse, V. Sauvant-Moynot, Comprehensive analyses of syntactic foam behaviour in deepwater environment, in: vol 44, Kluwer Academic Publishers, Van Godewijckstraat 30, Dordrecht, 3311 GZ, Netherlands, 2009, pp. 1462-1468.
[24] H. Mae, Materials Science and Engineering: A 496 (2008) 455-463.
[25] G. Subhash, Q. Liu, X.-L. Gao, International Journal of Impact Engineering 32 (2006) 1113-1126.
[26] H.S. Kim, H.H. Oh, Journal of Applied Polymer Science 76 (2000) 1324-1328.
[27] M. Hobbs, Journal of Thermal Analysis and Calorimetry 83 (2006) 91-95.
[28] R. Jhaver, H. Tippur, Journal of Reinforced Plastics and Composites 29 (2010) 3185-3196.
[29] B.L. Croop, Hubert, DYNAmore GmbH 7th European LS-DYNA Conference (2009).
[30] R. Abera, Finite Element Analysis of Interfacial Failure of Syntactic Foams Subjected to Uniaxial Compression, in: vol Master of Engineering, Southern University, 2010, p. 86.